Journal of Chemistry and Technologies, 2025, *33*(4), 1136-1148

Journal of Chemistry and Technologies

pISSN 2663-2934 (Print), ISSN 2663-2942 (Online).

journal homepage: http://chemistry.dnu.dp.ua
editorial e-mail: chem.dnu@gmail.com

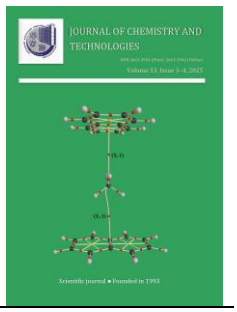

UDC 661.183.2:547.466.2:678.027.63

FLAME-RETARDANT BEHAVIOR OF UREA–METAPHOSPHORIC ACID COMPLEXES ON CELLULOSE-BASED MATERIALS

Gulyayra K. Kholikova[1], Uktam M. Mardonov[1], Bakhtiyor Sh. Ganiyev[1], Dilshoda A. Khazratova[1], Sevda H. Aliyeva[2], Muzafar S. Sharipov[1*]

[1]*Bukhara State University, M. Ikbol str. 11, 200117 Bukhara, Uzbekistan*
[2]*Nakhchivan State University, Dilgam Pishavari, Nakhchivan, AZ7012, Azerbaijan*
Received 7 Серпень 2025; accepted18 September September 2025; available online 25 December 2025

Abstract

In this study, novel urea metaphosphate complexes were synthesized at 1:1, 1:2, and 1:3 molar ratios using urea and metaphosphoric acid to obtain mono-, di-, and trimetaphosphate derivatives (UMP, UDP, and UTP). The synthesized compounds were comprehensively characterized through FTIR spectroscopy, powder X-ray diffraction (XRD), and elemental analysis, confirming their structural frameworks, protonation levels, and compositional features. Crystallographic analysis revealed distinct variations in unit-cell symmetry and packing as the phosphate chain length increased, indicating the formation of progressively more complex hydrogen-bonding networks. The flame-retardant performance of the complexes was examined using treated cellulose-based substrates, including paper, cardboard, and cotton fabric, in accordance with GOST R 50810-95 and GOST 12.1.004-91 standards. Experimental results demonstrated a clear enhancement in flame-retardant efficiency with increasing phosphate content, with UTP exhibiting the highest thermal stability and char-forming capability. Overall, the findings highlight the potential of urea metaphosphate complexes as multifunctional materials with promising applications in both agrochemistry and fire-protection technologies.

Keywords: urea metaphosphate; IR spectroscopy; XRD analysis; flame-retardant properties; phosphate complexes; cellulose materials.

ВОГНЕСТІЙКІ ВЛАСТИВОСТІ КОМПЛЕКСІВ СЕЧОВИНИ З МЕТАФОСФОРНОЮ КИСЛОТОЮ НА ОСНОВІ ЦЕЛЮЛОЗОВМІСНИХ МАТЕРІАЛІВ

Гуляйра К. Холікова[1], Уктам М. Мардонов[1], Бахтійор Ш. Ганієв[1], Ділшода А. Хазратова[1], Севда Г. Алієва[2], Музаффар С. Шаріпов[1]

[1]*Бухарський державний університет, вул. М. Ікбола, 11, 200117 Бухара, Узбекистан*
[2]*Нахічеванський державний університет, Ділгам Пішаварі, Нахічевань, AZ7012, Азербайджан*

Анотація

У цьому дослідженні було синтезовано нові комплекси метафосфатів сечовини у мольних співвідношеннях 1 : 1, 1 : 2 та 1 : 3 між сечовиною та метафосфорною кислотою з утворенням моно-, ди- та триметафосфатних похідних (UMP, UDP та UTP). Синтезовані сполуки були всебічно охарактеризовані методами Фур'є-інфрачервоної спектроскопії (FTIR), порошкової рентгеноструктурної дифракції (XRD) та елементного аналізу, що дозволило підтвердити їхню структурну організацію, ступінь протонування та елементний склад. Кристалографічний аналіз засвідчив суттєві відмінності у параметрах елементарної комірки та типах упаковки з підвищенням довжини фосфатного ланцюга, що вказує на формування більш розгалужених систем водневих зв'язків. Вогнезахисні властивості комплексів були досліджені на целюлозовмісних матеріалах (папір, картон, бавовняна тканина) відповідно до стандартів GOST R 50810-95 і GOST 12.1.004-91. Експериментальні дані показали зростання ефективності вогнезахисту зі збільшенням кількості фосфатних груп, причому комплекс UTP продемонстрував найвищу термостійкість і здатність до утворення захисного шару. Отримані результати підкреслюють перспективність метафосфатів сечовини як багатофункціональних матеріалів для агрохімії та вогнезахисних технологій.

Ключові слова: метафосфат сечовини; ІЧ-спектроскопія; рентгеноструктурний аналіз; антипіренові властивості; фосфатні комплекси; целюлозовмісні матеріали.

**Corresponding author*: *e-mail: sharipovms1981@gmail.com*

doi: 10.15421/jchemtech.v33i4.336986

Introduction

Agrochemical agents are used to supply plants with essential primary nutrients (nitrogen, phosphorus, and potassium) as well as secondary nutrients (calcium, magnesium, and sulfur). Nutrient-rich soil is required for plant growth and crop production. Chemical fertilizers play a crucial role in various sectors of agriculture, particularly in intensive farming systems aimed at achieving high yields, and are applied to meet the nutritional needs of crops in soils that cannot provide sufficient amounts of nutrients rapidly and in their natural state [1–4].

Urea phosphate (UP) is a molecular salt composed of carbon, hydrogen, nitrogen, oxygen, and phosphorus. Its chemical formula is $[CO(NH_2)_2{\cdot}H_3PO_4]$. It is a dry, white crystalline substance with a melting point of 117.3 °C and contains 17.7 % nitrogen (N) and 44.6 % P_2O_5. Urea phosphate is acidic, highly soluble in water (960 g/L at 20 °C), and has a specific gravity of approximately 1.76 g/cm^3. Its critical humidity at 30 °C ranges between 75 % and 80 %, similar to that of urea. Agrochemical testing [5] has shown that this compound is a valuable product, used as a ready-to-apply fertilizer and as an intermediate in the production of polyphosphate-based solid and liquid fertilizers. Urea phosphate is often employed for cleaning pipeline systems and for drip irrigation of crops [6]. Furthermore, it has been successfully used as a specialized cleaning agent and as an active ingredient in certain detergent formulations. Additionally, reports indicate its application in animal husbandry as a dietary supplement for cattle [7].

In urea phosphate production, urea and orthophosphoric acid (H_3PO_4) are used as the primary raw materials. This acid is obtained through the wet process and represents technical-grade orthophosphoric acid containing various impurities. These impurities primarily consist of dissolved organic and inorganic substances originating from the physical and chemical processing of phosphate minerals, the reaction process with sulfuric acid, and the technological equipment and methods employed [8]. The relative content of these impurities can vary significantly depending on the types of raw materials and the technological processes used by manufacturers. Excessive levels of impurities in phosphoric acid lead to several adverse effects, including the formation of undesirable colored precipitates and scaling, as well as changes in the viscosity, density, and other physical properties of the slurry [9].

One of the main challenges in urea phosphate production is the structural instability and low quality of phosphoric acid obtained via the wet process. In particular, solid particles and impurities in the raw material adversely affect the color of the product crystals and the clarity of the solution. To address this issue, a two-stage technological reactor system based on the wet dihydrate process has been developed. In this process, phosphoric acid is obtained through the reaction of phosphate raw materials with gypsum and sulfuric acid [10].

After leaving the second reactor, the product mixture containing various impurities is directed into a column-type reactor, where gypsum crystallizes. It then reacts with phosphoric acid in a 1.0–1.1 molar ratio. The resulting mixture is separated from gypsum using a centrifuge and directed to a cooling tower. Subsequently, it is treated with 1 % sulfuric acid, during which urea phosphate crystals are formed in hydrocyclones. These crystals are separated by centrifugation and dried in a hot-air stream. The solution is then re-concentrated using a special concentration system, which involves partial recirculation of the main solution. This process allows efficient separation of urea phosphate crystals and precipitation of impurities [11].

The production of urea phosphate involves mixing 36–85 % phosphoric acid with urea in a 1.0–1.4 molar ratio at 60–100 °C in the presence of activators and stabilizers. The reaction mixture is concentrated under pressure, and the resulting crystals are cooled to 30–40 °C and dried. Using Jordanian phosphoric acid, an industrial-scale technology for producing urea phosphate with a composition of 17-44-0 ($N–P_2O_5–K_2O$) has been developed, and the parameters of the crystallization process have been evaluated [12].

The thermal decomposition of urea phosphate has been studied using density functional theory (DFT), revealing the formation of ammonium dihydrogen phosphate and other phosphates. The study identified key kinetic parameters and reaction mechanisms important for fertilizer production [13]. DFT calculations have also shown that certain bis-urea-based receptors exhibit strong binding affinity for phosphate anions, and this binding can be controlled through photoisomerization [14]. Another study using DFT demonstrated that molecular interactions in a stiff-stilbene-based receptor can either inhibit or enhance phosphate binding depending on the isomeric state [15]. Additionally, DFT analysis of a tripodial tris(urea) receptor explained how its

binding states with phosphate anions influence its fluorescence properties [16].

Moreover, compounds of urea not only with phosphoric acid but also with nitric acid have been extensively studied by several researchers [17–20]. In 1943, a U.S. patent was issued for the synthesis of nitrourea (NU) [21]. The physical properties of NU and urea nitrate (UN) have been compared, revealing that these are distinct compounds with differing composition, structure, and properties: nitrourea (NU) is a nitro derivative of urea with substituted nitrogen, while urea nitrate (UN) is the nitrate salt of urea, forming a molecular complex [22]. The synthesis, structure, and properties of urea–formaldehyde resins and other urea-based sorbents, corrosion inhibitors, and adhesive compositions have also been investigated [23–25].

Kh. I. Akbarov et al. synthesized water-soluble composite inhibitors based on the urea–phosphoric acid adduct. Their inhibitory effects on St-3 steel alloys were studied using a Corroziometer CE 105. The results showed that the corrosion inhibition efficiency (K) of urea phosphate reached 16.93 g/(m²·h) after 360 h and 11.10 g/(m²·h) after 720 h, with corresponding protection efficiencies (Z) of 87.15 % and 89.23 % [28; 29].

The reviewed literature indicates that only the properties of urea compounds with orthophosphoric acid have been studied and applied for various purposes. However, the structures and properties of urea molecular complexes with metaphosphoric acid have not been investigated. In this study, the authors report the synthesis, structure, and properties of urea mono-, di- and trimetaphosphate complexes. Specifically, infrared (IR) spectroscopy and X-ray diffraction (XRD) were employed to study their structures. Furthermore, the flame-retardant efficiency of the synthesized complexes was also evaluated.

Materials and methods

Materials and preparations of complexes

Urea (carbamide, amide of carbonic acid) $(NH_2)_2CO$ – crystal. T_m=132.7 °C, soluble in water, enters alcohols and liquid NH_3 and CO_2 according to the Bazarov reaction (saves 46 % N). Urea is produced locally in "Navoiazot" JSC.

Metaphosphoric acid (~65 % HPO_3 basis) – chemically pure grade, supplied by Sigma-Aldrich (Germany). It is a polymeric acid with the general formula $(HPO_3)_n$, appearing as a white, glassy substance. The compound is hygroscopic and exhibits strong acidic properties. It dissolves slowly in cold water but readily in heated water.

In studying the flame-retardant efficiency of the synthesized compounds, fabric, paper, and cardboard samples were used.

Synthesis of urea metaphosphate complexes

A total of 18 g (0.3 mol) of urea and 24 g (0.3 mol) of colorless crystalline metaphosphoric acid (M_r = 80 g/mol) were used. The metaphosphoric acid was first dissolved in 100 mL of distilled water, after which urea was added, and the solution was stirred at 40 °C. Evaporation was carried out at 110–120 °C. The resulting white crystalline product was hygroscopic, with a yield of 34.44 g (82 %) (Table 1). The reaction equation is as follows:

$$CO(NH_2)_2 + HPO_3 \rightarrow [(NH_2)_2CO{\cdot}H^+]PO_3^-.$$

Using the same procedure, by increasing the amount of metaphosphoric acid, syntheses were carried out at molar ratios of 1:2 (51.02 g, 77.3 %) and 1 : 3 (84.6 g, 94 %). The reaction equations are:

$$CO(NH_2)_2 + 2HPO_3 \rightarrow [(NH_2)_2CO{\cdot}H_2^{2+}](PO_3^-)_2$$
$$CO(NH_2)_2 + 3HPO_3 \rightarrow [(NH_2)_2CO{\cdot}H_3^{3+}](PO_3^-)_3.$$

Table 1

Physicochemical properties of urea metaphosphate complexes

№	Compounds	χ, 25° C, mS/sm	Color	Yield	$T_{suyuq.}$	Found (%)			Calculated (%)		
				%	^{0}C	C	H	N	C	H	N
1	Urea monometaphosphate (UMP)	42.3	White	82	152.4	8.58	3.60	20.01	8.61	3.23	19.8
2	Urea dimetaphosphate (UDP)	61.8		77.3	164.8	5.46	2.75	12.73	5.47	2.71	12.52
3	Urea trimetaphosphate (UTP)	75.4		94	176.2	4.00	2.35	9.34	4.01	2.24	4.00

The above syntheses demonstrate that the reactions of urea with nitric and metaphosphoric acids result in the formation of hygroscopic, water-soluble complexes with varying degrees of protonation. In both groups, an increase in acid content leads to enhanced protonation, as well as a consistent rise in melting temperature and electrolytic conductivity. Phosphate complexes are more stable than their nitrate counterparts but exhibit lower conductivity. These variations

are attributed to the number of ions, the degree of protonation, and the type of acid residues present in the complex structures.

Methods

Powder X-ray Diffraction Analysis – Structural characterization of the compound was performed using a Malvern Panalytical Empyrean powder diffractometer. The XRD measurements employed CuKα radiation (λ = 1.54 Å). The generator was operated at an accelerating voltage of 45 kV and an emission current of 40 mA [29; 30]. Diffraction patterns were collected in the 2θ range of 20°–120° using Bragg–Brentano geometry with a constant scan rate of 0.33°/min. The obtained diffraction data were processed using the Profex software, and the crystalline phases present in the samples were identified [30].

IR spectral analysis – the IR spectra of the synthesized complex compounds were recorded using an "IRTracer-100" spectrometer (Shimadzu, Japan) equipped with a MIRacle-10 attenuated total reflectance (ATR) accessory with a diamond/ZnSe prism. The spectra were obtained in the range of 4000–500 cm^{-1}, with a resolution of 4 cm^{-1} and a signal-to-noise ratio of 60.0:1.

Elemental analysis – the C, H and N elemental composition of the complexes was determined at L.N. Gumilyov Eurasian National University using a "EuroVector EA3000 Series CHNS-O Elemental Analyzer" (EuroVector, EU). The results are presented in Table 1 [31].

Determination of sample mass loss in air (fire-tube method).

The "fire-tube" method is a rapid technique for determining the flammability group of solid combustible materials. It is carried out in accordance with State Standard GOST- 12.1.004-91. The apparatus consists of a combustion chamber, a sample holder, a gas burner with a diameter of 7 mm, and a movable glass screen with a diameter of 50 mm mounted on a stand. The combustion chamber is a vertically mounted tube with a diameter of (50±3) mm, a length of (165±5) mm, and a wall thickness of (0.5±0.1) mm. For testing, six samples are prepared with dimensions not exceeding (35±1) mm in width, (150±3) mm in length, and (10±1) mm in thickness.

Pre-weighed samples are placed vertically in the center of the tube so that their ends protrude by 5 mm and are positioned 10 mm above the gas burner. A burner with a flame height of (40±5) mm is placed beneath the central part of the sample, and a stopwatch is started simultaneously to record the burning time required for stable ignition. After 2 minutes of flame exposure, the ignition source is removed, and the duration of the sample's independent burning and smoldering is measured. Once the sample has cooled to room temperature, its mass is measured, and the mass loss (m) is determined as a percentage relative to the initial mass using the following formula:

$$m = \frac{M_n - M_k}{M_k} \times 100 \quad (1)$$

where M_n and M_k are the sample masses before and after testing (g), respectively.

Results and discussion

X-ray phase analysis of Urea metaphosphate complexes

At National Technical University Kharkiv Polytechnic Institute (Kharkiv Polytechnic Institute), Associate Professor Yu.I. Vetsner studied the formation process of urea phosphate using two types of orthophosphoric acid - "technical grade" and "analytical grade" - as well as urea of the superior, first, and second grades. The individuality of the resulting samples was confirmed by examination on a "Siemens D 500" diffractometer within the angular range of $20 \le 2\theta \le 60°$ [32; 33]. For the analysis of the diffractograms, the Voigt function was applied using the WinPLOTR and FullProf software packages [34; 35]. The X-ray diffractograms are presented in Figures 1 and 2.

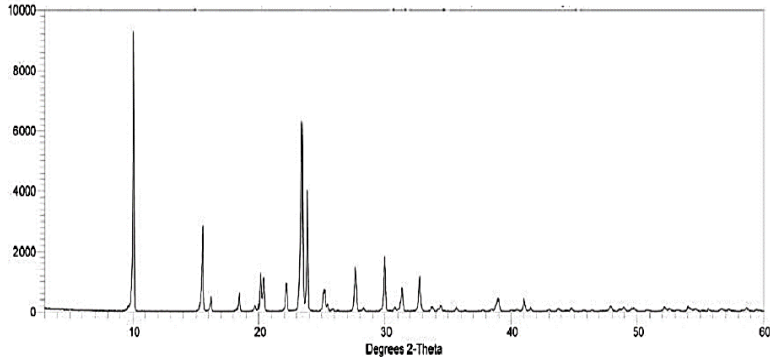

Fig. 1. X-ray diffractogram of the salt synthesized from H_3PO_4 and urea [32].

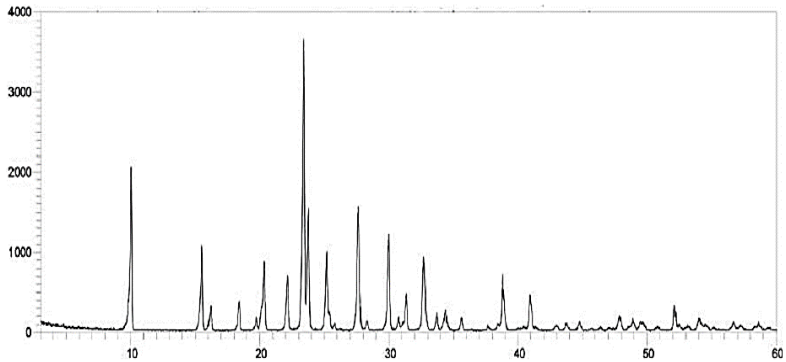

Fig. 2. X-ray diffractogram of the urea salt synthesized using technical-grade H_3PO_4 [33].

However, unlike the above-mentioned study, the X-ray phase analysis of urea monometaphosphate and dimetaphosphate complexes was carried out using the reflection lines (peaks) observed in the diffractograms (Fig. 3, 4). This made it possible to determine and analyze the particle sizes, as well as the parameters of each initial component and the resulting products within their composition. In addition, these samples were examined to establish the quantitative ratios of the amorphous and crystalline phases of urea and urea phosphate, their elemental composition, and their properties by comparing them with various crystalline structures from the database using the Expo2014 software (Table 2).

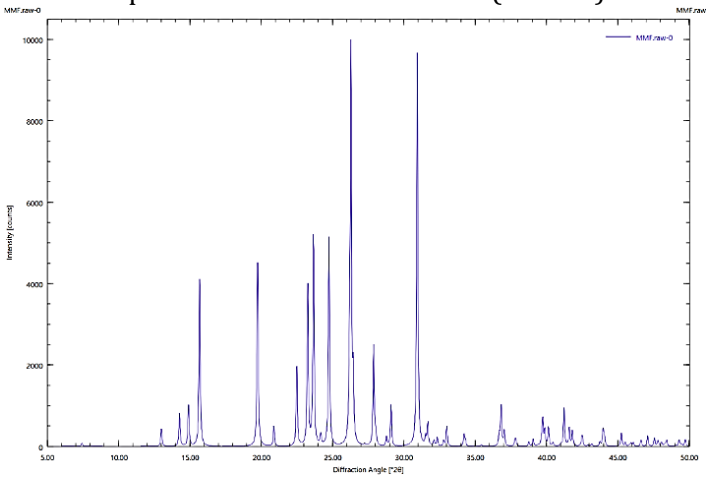

Fig. 3. X-ray diffractogram of the UMP

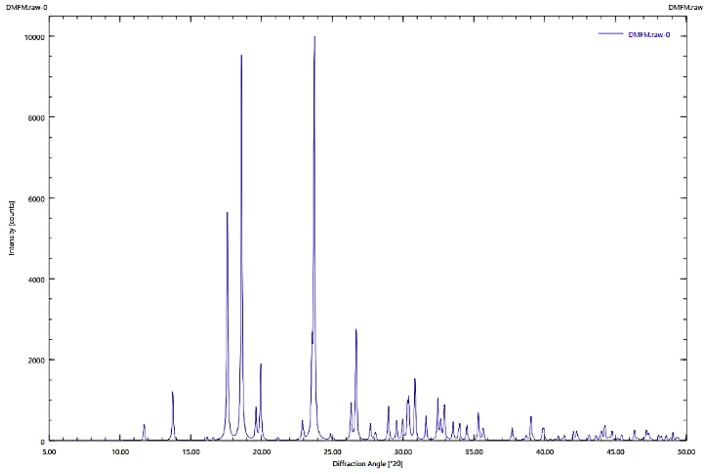

Fig. 4. X-ray diffractogram of the UDP

The crystallographic analysis reveals significant structural differences among the studied complexes. The urea monometaphosphate (UMP) crystallizes in an orthorhombic system (Pnma), whereas the di- (UDP) and trimetaphosphate (UTP) complexes adopt monoclinic ($P2_1/c$) and trigonal (P3) crystal systems, respectively (Table 2).

Table 2

Journal of Chemistry and Technologies, 2025, *33*(4), 1136-1148

Crystallographic parameters of urea molecular complexes with mono-, di-, and trimetaphosphates (UMP, UDP, and UTP).

Parameter	Complexes		
	UMP	**UDP**	**UTP**
Crystal system	Rhombic	Monoclinic	Trigonal
Spatial group	Pnma	$P2_1/c$	$P\bar{3}$
a (Å)	7.9142(3)	9.3687(4)	8.5891(2)
b (Å)	5.2563(2)	6.7431(3)	8.5891(2)
c (Å)	11.1789(4)	12.9125(5)	14.2574(4)
β (°)	90	105.127(2)	90
V (Å^3)	464.83(3)	791.54(6)	910.85(4)
Z	4	4	4
ρ_{calc} (g/cm^3)	2.018	2.235	2.341
R_1 [I>2σ(I)]	0.0287	0.0312	0.0298

The cell dimensions indicate an increase in unit cell volume from 464.83 Å^3 for UMP to 910.85 Å^3 for UTP, reflecting the higher molecular content in the latter. The density values (2.018–2.341 g/cm^3) show a gradual increase with the complexity of the phosphate anion. The refinement indicators (R_1 < 0.03) confirm good reliability of the structural models (Tabel 2). These crystallographic features correlate with the nature of the phosphate ligands and the hydrogen-bonding network within the complexes.

IR spectroscopy of complexes

Analysis of the metaphosphoric acid spectrum shows that the weak bands with maxima at 3574.1 cm^{-1} and 1645 cm^{-1} are attributed to the ν(OH) and δ(HOH), δ(HOP) vibrations, indicating the presence of a non-bonded OH group in its structure (Fig. 5). The broad band observed in the 2600–3200 cm^{-1} range, with a maximum at 2737.0 cm^{-1}, is associated with the vibrations of the hydrogen-bonded OH group of HPO_3 and water. The group of weak-intensity bands in the range of 1600–1560 cm^{-1}, with a shoulder at 1558.48 cm^{-1}, is cautiously assigned to the deformation vibrations δ(HOH) and δ(HOP) of hydrogen-bonded groups [36]. These data suggest that in metaphosphoric acid, its molecules are strongly associated through the formation of intermolecular hydrogen bonds, both among themselves and with water molecules. In the region corresponding to the characteristic absorption bands of the metaphosphate ion (PO_3^-), several bands are observed at 1257.6, 1165.0, and 1072.42 cm^{-1}, along with a broad medium-intensity band at 939.33 cm^{-1} and a weak band at 740.67 cm^{-1}. These bands are associated with the ν_{as}(P–O), ν_s(P–O), ν_{as}(P=O), and δ(O–P–O) vibrations, respectively (Fig. 5) [37].

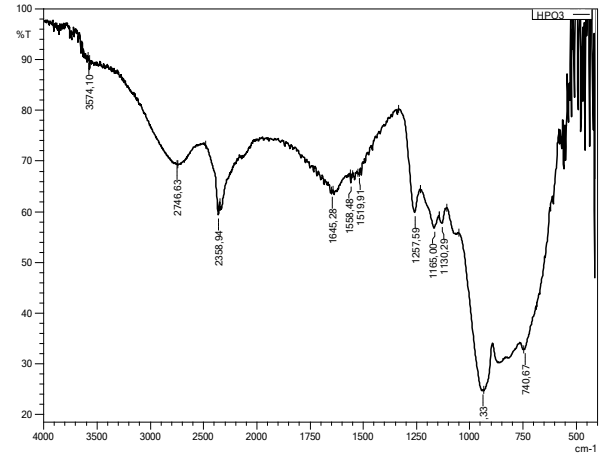

Fig. 5. IR spectra of HPO_3

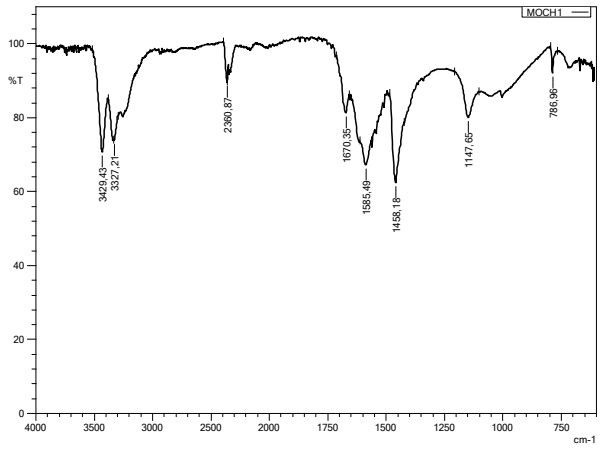

Fig. 6. IR spectra of $CO(NH_2)_2$

Upon interaction with urea molecules in a 1:1 molar ratio of HPO_3:$CO(NH_2)_2$, an adduct is formed, likely involving the NH_2 group of urea and the OH group of HPO_3. This is evidenced by the disappearance of the weak band at 3574.10 cm^{-1} and the reduced intensity of the broad band centered at 2737.0 cm^{-1}. Additionally, the ν_s(NH) band of urea exhibits an anomalous high-frequency shift (+7.7 cm^{-1}) (Fig. 6, 7). The characteristic absorption bands corresponding to the ν(C=O) and ν(C–N) vibrations remain unchanged, while the number of bands associated with the metaphosphate group is reduced. Specifically, among the bands observed in the spectrum of the free acid, only a single medium-intensity band at 964.71 cm^{-1} (ν(P=O)) appears.

This likely indicates the involvement of oxygen atoms from the PO_3^- group in interactions with the hydrogen atoms of the NH_2 group of urea. The results of the IR spectral analysis suggest a linear chain polymeric structure for the metaphosphoric acid–urea adduct in a 1 : 1 ratio. The proposed structure of the $CO(NH_2)_2 \cdot HPO_3$ (UMP) salt can be represented as follows: Scheme 1.

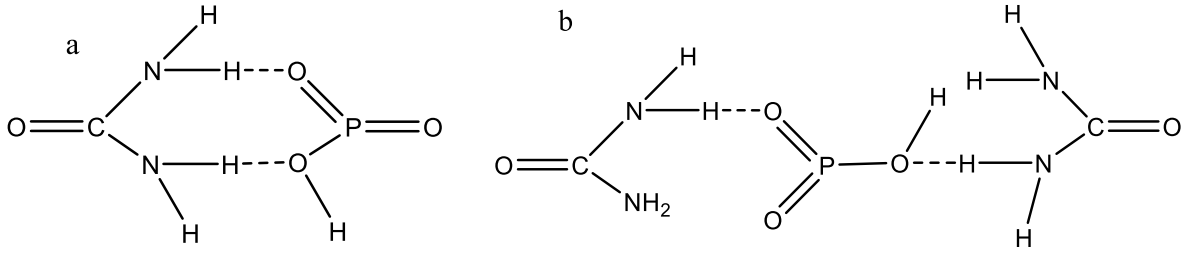

Scheme 1. Proposed hydrogen-bonded structures of urea metaphosphate complexes: (a) Monomeric structure of $CO(NH_2)_2 \cdot HPO_3$ (UMP) showing intramolecular hydrogen bonding; (b) Extended hydrogen-bonded network involving two urea molecules and one metaphosphate group

The spectrum of the salt obtained at a $CO(NH_2)_2 : HPO_3$ molar ratio of 1 : 2 exhibits significant differences compared to the spectra of the starting materials and the 1 : 1 adduct. The absorption bands corresponding to the asymmetric and symmetric N–H stretching vibrations are markedly reduced in intensity and appear as a weak doublet, undergoing a low-frequency shift to (ν_{as}(N–H) 3327.2 cm^{-1} and ν_s(N–H) 3203.76 cm^{-1}), with shifts of 57.86 and 123.44 cm^{-1}, respectively.

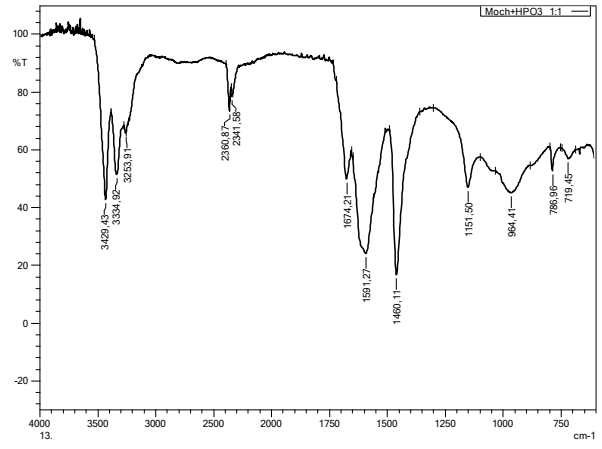

Fig. 7. IR spectra of UMP

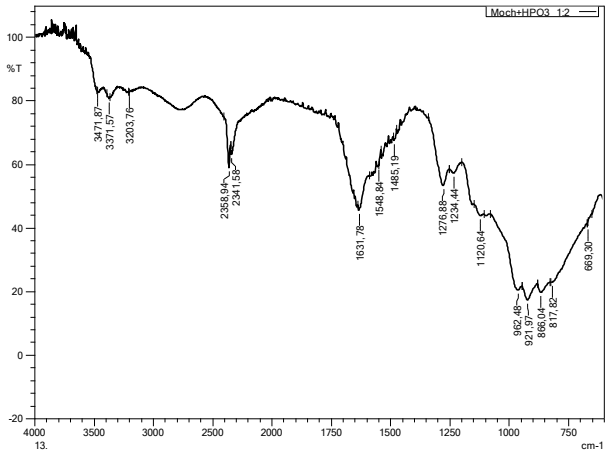

Fig. 8. IR spectra of UDP

A detailed analysis of the N–H band manifestations in the spectra of the free acid, the 1 : 1 adduct, and the 1 : 2 complex with metaphosphoric acid reveals changes in the frequency interval (i.e., the difference between ν_{as} and ν_s of the N–H bands) of the urea amino group (Fig. 8, 10). These values are as follows: $\Delta\nu_{(N-H)(urea)}$=102.3; $\Delta\nu_{(N-H)(UMP)}$=94.5 and $\Delta\nu_{(N-H)(UDP)}$ =167.81 cm^{-1}.

Although a definitive interpretation of these observations has not yet been established, it is tentatively suggested that the NH_2 group is involved to different extents and in different bonding environments in the formation of the $CO(NH_2)_2 \cdot HPO_3$ adducts. This assumption is further supported by the behavior of the ν(C=O), ν(C–N), and δ(NH_2) absorption bands. In the spectra of urea and the 1 : 1 HPO_3 adduct, the characteristic bands of these vibrations are nearly identical, indicating that the C=O group does not participate in salt formation at this ratio.

In contrast, in the spectrum of the UDP, the typical three bands at 1670, 1586 and 1458 cm^{-1} are replaced by a broad, intense band spanning the range 1750–1450 cm^{-1}, with a maximum at 1631.78 cm^{-1} and shoulders at 1580 and 1475 cm^{-1}. These spectral changes suggest that both the C=O and NH_2 groups of urea are involved in the formation of the 1:2 complex (UDP).

The absorption band at 1257.6 cm^{-1} in the spectrum of HPO_3 is attributed to the $\nu_{as}(PO_2)$ vibration, while the bands at 1165.0 cm^{-1} and 1105.0 cm^{-1} correspond to ν_s(P–O_2). The band at 1072 cm^{-1} is associated with the ν_as(P–O–P) vibration, and the one at 740.87 cm^{-1} with ν_s(P–

O–P). A weak band at 808 cm^{-1} is assigned to the out-of-plane deformation vibration δ(POP).

It is noteworthy that intermolecular attractive forces between $CO(NH_2)_2$ and HPO_3 molecules in the resulting product arise through weak interactions between the NH_2 group and the P=O group. This is evidenced by the anomalous high-frequency shift of 7.0 cm^{-1} in the ν_s(N–H) band of urea and the absence of a series of bands characteristic of ν(P–O_2). However, the reason for this disappearance remains unexplained.

When the $CO(NH_2)_2$: HPO_3 ratio is increased to 1:2, another compound, presumably of adduct character, is formed. However, the IR spectrum of this compound differs significantly from that of the $[CO(NH_2)_2 \cdot HPO_3]$ adduct. In the high-frequency region, three absorption bands of relatively low intensity appear, in contrast to the corresponding stronger bands in the spectrum of pure urea (Fig. 6, 9). The first band at 3471.87 cm^{-1} and a broad band centered at 3740.0 cm^{-1} are attributed to ν(O-H) stretching vibrations involved in intermolecular hydrogen bonding with the oxygen atoms of the PO_3^- groups of metaphosphoric acid. The remaining two bands at 3371.57 cm^{-1} and 3203.76 cm^{-1} correspond to the ν_{as}(N–H) and ν_s(N–H) vibrations of the amino group, indicating its participation in interactions with HPO_3 molecules.

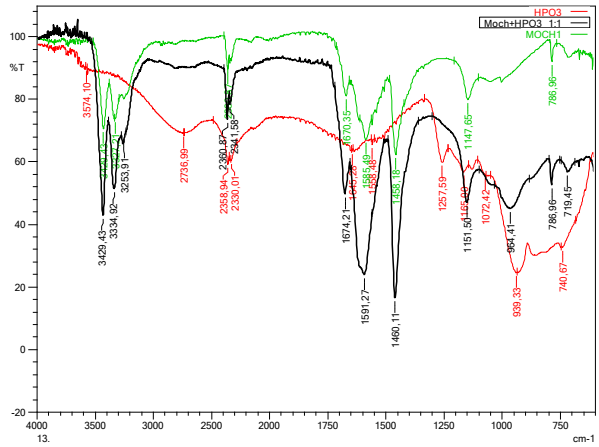

Fig. 9. Comparative IR spectra of UMP, urea and metaphosphoric acid

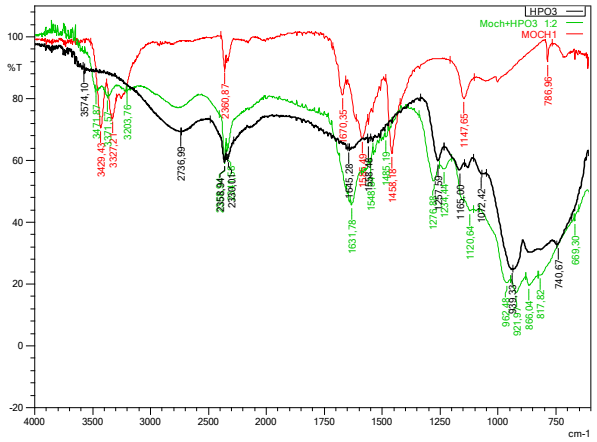

Fig. 10. Comparative IR spectra of UDP, urea and metaphosphoric acid

Similar changes are observed in the 1700–1500 cm^{-1} region of the spectrum, where the ν(C=O), ν(C–N), and δ(NH_2) vibrations of urea typically appear. In the spectrum of the investigated compound, these three distinct bands are merged into a single broad, intense band with a maximum at 1631.76 cm^{-1} and inflection points at 1548.54 and 1485.19 cm^{-1}. This suggests the involvement of both the C=O and NH_2 groups of urea in the formation of a molecular complex with the composition $[CO(NH_2)_2 \cdot 2HPO_3]$, presumably featuring one of the two cyclic structures proposed below Scheme 2.

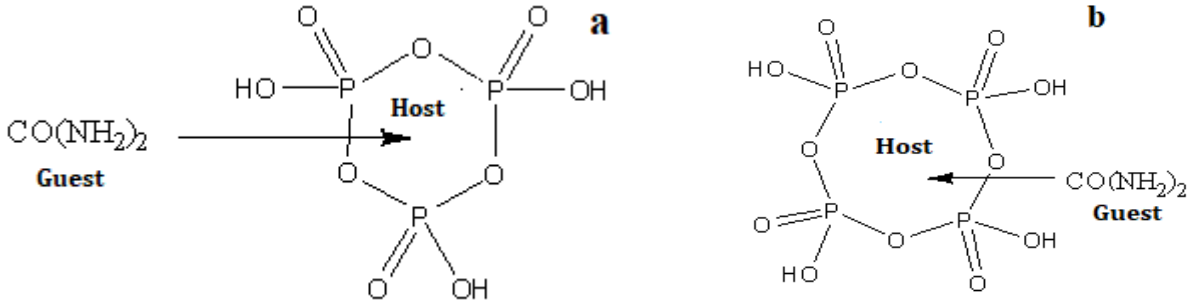

Scheme 2. Proposed cyclic structures of the $[CO(NH_2)_2 \cdot 2HPO_3]$ molecular complex, indicating host–guest interaction via the urea's C=O and NH_2 groups with the metaphosphoric acid framework:
(a) Interaction model with inward-directed urea; (b) Alternative model with outward-directed urea molecule

Flame-retardant efficiency of urea complexes

Flame-retardant properties of urea (U) and metaphosphoric acid (MP) on various materials

To evaluate the flame-retardant properties of urea (U) and metaphosphoric acid (MP), solutions of the substances were first prepared at a known concentration (1 M). Two samples (150 × 50 mm),

each of calico fabric, paper, cardboard, and wood, were prepared, and their initial masses were measured. The samples were then impregnated with 10, 20 and 50 ml portions of the prepared solutions for a duration of 2 hours. After impregnation, the samples were air-dried at room temperature (20 °C) for 24 hours, followed by thermal treatment at 180 °C for 15 minutes.

The treated samples were then subjected to flame testing according to the requirements of GOST R 50810-95 and GOST- 12.1.004-91. The results are presented in Table 3.

Table 3

Flame-retardant test results of urea and metaphosphoric acid on paper, cardboard and cotton fabric samples

№	Substance	Temp (°C)	Initial Mass (g)	Treated Mass (g)	Burning Time (s)	Residual Mass (g)	Flame Retardancy (%)	Volume (mL)
1	U	Paper	0.6461	0.6985	0	-	10 ml	8-10
2	MP	Paper	0.6521	0.7021	0.3498	53.6420	10ml	4
3	U	Cardboard	6.7256	7.1989	4.8300	71.8151	20ml	2
4	MP	Cardboard	7.7694	7.2925	5.9354	76.3945	20ml	3
5	U	cotton fabric	1.3587	1.5529	0.7084	52.1380	10ml	2
6	MP	cotton fabric	1.3565	1.6632	1.2174	89.7456	10ml	1

The experimental data show that metaphosphoric acid exhibits superior flame-retardant efficiency compared to urea on all tested materials. For paper and cotton, MP-treated samples retained significantly more mass after combustion and demonstrated higher flame retardancy percentages (up to 96.78 %). Notably, the residual mass of MP-treated cardboard and fabric indicates effective char formation, which contributes to fire resistance. Wood samples did not show quantifiable results due to high variability or incomplete combustion, warranting further testing. Overall, MP demonstrates more stable and effective thermal protection than U (Table 3).

Experimental results of flame-retardant properties of urea metaphosphate complexes on paper samples.

Six paper samples (150 × 50 mm) were prepared and weighed. Each sample was soaked in 10 mL of urea phosphate solutions: urea monometaphosphate (UMP), urea dimetaphosphate (UDP), and urea trimetaphosphate (UTP), for 2 hours. After soaking, the samples were dried at 20 °C for 24 hours. Some of the samples were then thermally treated at 180 °C for 15 minutes, and their masses were recorded. The samples were ignited according to GOST- 12.1.004-91standards (Figure 13). The results are given in Table 4.

Table 4

Flame-retardant test results of urea metaphosphate complexes on paper samples

№	Substance	Temp (°C)	Initial Mass (g)	Treated Mass (g)	Burning Time (s)	Residual Mass (g)	Flame Retardancy (%)	Volume (mL)
1	UMP	20	0.6226	0.7306	1	0.4255	58.2398	50
2	UDP	20	0.6416	0.7443	2	0.4097	55.0450	50
3	UTP	20	0.6271	0.8397	_	0.7444	88.6507	50
4	UMP	80	0.6517	0.7052	1	0.4960	70.3346	50
5	UDP	80	0.6741	0.7680	2	0.4213	54.8567	50
6	UTP	80	0.6759	0.8716	_	0.8354	95.8467	50
7	Untreated		0.6782	0.6782	6-7	_	0	-

The results reveal that UTP (urea trimetaphosphate) displays the highest flame-retardant efficiency, particularly after thermal treatment at 80 °C, achieving 95.85 % retardancy. At room temperature, UTP also outperforms UMP and UDP, suggesting that the number of metaphosphate units positively correlates with flame-retardant performance (Fig. 11). Thermal pretreatment generally enhances the retention of mass post-combustion, likely due to improved binding and stabilization within the cellulose matrix. UMP and UDP showed moderate effects, while untreated samples completely burned within 6–7 seconds, highlighting the necessity of treatment.

Fig. 11. Flame-retardancy test on paper samples

Experimental results of flame-retardant properties of urea metaphosphate complexes on cardboard samples

Six cardboard samples (150 × 50 mm) were prepared and weighed. Each was soaked in 20 mL of UMP, UDP, and UTP solutions for 2 hours. After drying at 20 °C for 24 hours, a portion of the samples was heat-treated at 180 °C for 15 minutes (Fig. 12). The samples were then ignited as per GOST- 12.1.004-91. Results are presented in Table 5.

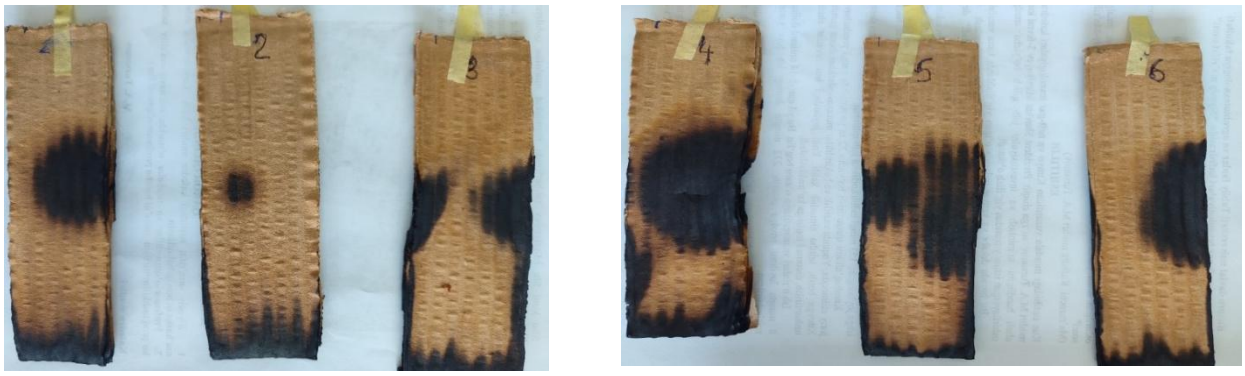

Fig. 12. Flame-retardancy test on cardboard samples

Cardboard samples treated with UDP and UTP exhibited excellent flame-retardant behavior, with residual masses after burning exceeding 90 % (Table 5). The best performance was observed with UTP at 80 °C, indicating that both phosphate chain length and thermal activation contribute synergistically to fire resistance. Compared to UMP, both UDP and UTP formed a more stable and protective barrier during combustion. Untreated samples showed only 50.45 % retardancy and burned for 35–45 seconds, confirming the efficacy of urea metaphosphate complexes in enhancing fire resistance in cellulose-based substrates.

Table 5

Flame-retardant test results of urea metaphosphate complexes on cardboard samples

No	Substance	Temp (°C)	Initial Mass (g)	Treated Mass (g)	Burning Time (s)	Residual Mass (g)	Flame Retardancy (%)	Volume (mL)
1	UMP	20	6.5571	7.8359	1	6.9122	88.2119	100
2	UDP	20	7.0260	8.4846	2	7.7935	91.8546	100
3	UTP	20	7.1211	9.7768	1	8.8977	91.0083	100
4	UMP	80	6.7219	7.9990	1	6.7372	84.2255	100
5	UDP	80	6.4985	7.6030	1	7.0168	92.2898	100
6	UTP	80	6.6315	8.7671	1	8.1586	93.0592	100
7	Untreated		8.7875	8.7575	35-45	4.4181	50.4493	_

Experimental results of flame-retardant properties of urea metaphosphate complexes on cotton fabric samples

Six cotton fabric samples (100 × 50 mm) were prepared and weighed. Each sample was soaked in 10 mL of UMP, UDP, and UTP solutions for 2 hours. After drying at room temperature (20 °C) for 24 hours, some were heat-treated at 180 °C for 15 minutes (Fig. 13). The samples were ignited according to GOST R 50810-95. Results are presented in Table 6.

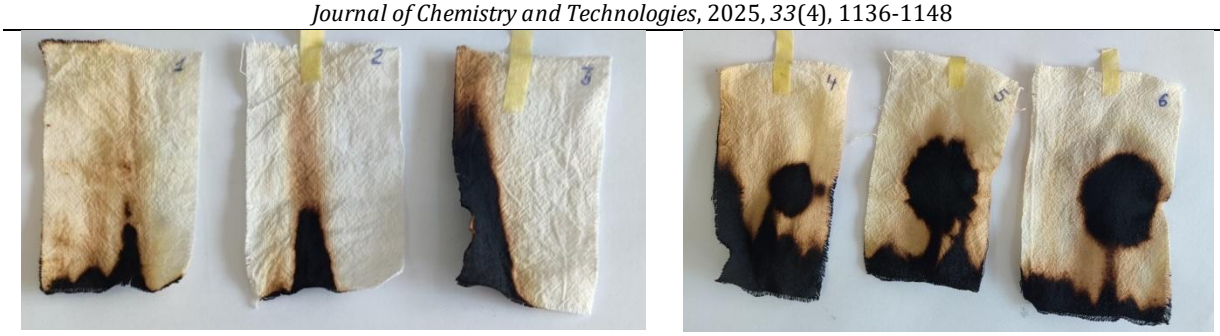

Fig. 13. Flame-retardancy test on cotton fabric samples

Cotton fabric samples treated with UDP achieved the highest flame-retardant performance at room temperature (96.78 %), followed closely by UMP and UTP. Interestingly, while all treated samples showed 0-second ignition (no visible flame spread), UMP performed less effectively after thermal pretreatment. This suggests that excess thermal curing may reduce the bonding efficiency of some lower-order phosphates with cotton. In contrast, UTP-treated samples maintained good performance regardless of temperature, likely due to more extensive hydrogen bonding and molecular cross-linking. Untreated fabric samples were fully combusted within 5–10 seconds.

Table 6

Flame-retardant test results of urea metaphosphate complexes on cotton fabric samples

No	Substance	Temp (°C)	Initial Mass (g)	Treated Mass (g)	Residual Mass (g)	Flame Retardancy (%)	Volume (mL)	Burning Time
1	UMP	20	0.9916	1.2749	1.1768	92.3952	50	0
2	UDP	20	1.0133	1.3985	1.3535	96.7822	50	0
3	UTP	20	0.9962	1.7231	1.4667	85.1198	50	0
4	UMP	80	0.9947	1.3240	0.9665	72.9984	50	0
5	UDP	80	1.0468	1.4586	1.1832	81.1118	50	0
6	UTP	80	1.3037	2.1322	1.7725	83.1301	50	0
7	Untreated	20	1.0578	1.0578	–	0	–	

Conclusion

This research presents the successful synthesis and characterization of new urea metaphosphate complexes, offering valuable insights into their physicochemical and structural properties. The experimental results confirmed that increasing the phosphate-to-urea molar ratio enhances protonation and thermal stability, as reflected in both IR and XRD data. Crystallographic analysis revealed a progression from orthorhombic to monoclinic and trigonal systems as phosphate content increased. The flame-retardant testing demonstrated that the UTP complex (urea trimetaphosphate) exhibited superior fire resistance on paper, cardboard, and cotton substrates, outperforming monometaphosphate and dimetaphosphate analogs. These findings suggest that such complexes may serve not only as efficient flame retardants but also as promising candidates for use in multifunctional agrochemical formulations. Future studies may further investigate their environmental safety, biodegradability, and synergistic effects with other additives.

References

[1] Jones, R.W. (1987). *Organic facies*. In: Welte D, ed. Advance in Petroleum Geochemistry. London: Academic Press. 1–89.

[1]. Gopp, N. V. (2021). The influence of agrochemicals on spatiotemporal changes in the agrochemical properties of the soil and the yield of broccoli. *Soils and the Environment, 4*(2), e157. https://doi.org/10.31251/pos.v4i2.157

[2]. Salvagiotti, F., Castellarín, J., Pedrol, H., Dignani, D. (2010). *Cations and phosphorus changes and budgets in a long term fertilization experiment on an Argiudol soil in Argentin*a. In Proceedings of the 19th World Congress of Soil Science: Soil Solutions for a Changing World.

[3]. Makhkamova, A., Kamilov, B. (2023). Importance of humine preparation and organic fertilizers in improving the fertility of eroded typical gray soils. *E3S Web of Conferences*. https://doi.org/10.1051/e3sconf/202337602015

[4]. Gasser, J.K. R., Penny, A. (1967). The value of urea nitrate and urea phosphate as nitrogen fertilizers for grass and barley. *The Journal of Agricultural Science, 69*(1), 139–148. https://doi.org/10.1017/S0021859600016555

[5]. Kilmer, V.J. (1980). Fertilizers of the future and factors affecting their role in crop production. *Agrochemicals in Soils. Pergamon*, 3–10. https://doi.org/10.1016/B978-0-08-025914-7.50004-9

[6]. Kiiskinen, T. (1983). Effects of Regent rapeseed meal fed during the rearing and laying period on the performance of chickens. *Ann. Agric. Fenn., 22*, 221–231.

[7]. Feki, M., Chaabouni, M., Ayedi, H. F., Heughebaert, J.C., Vaillant, M. (1987) Statistical analysis of the removal of aluminum and magnesium impurities from wet-process phosphoric acid. *The Canadian journal of chemical engineering, 65*(1), 132–136. https://doi.org/10.1002/cjce.5450650121

[8]. El-Asmy, A.A., Serag, H.M., Mahdy, M.A., Amin, M.I. (2008). Purification of phosphoric acid by minimizing iron, copper, cadmium and fluoride. *Separation and Purification Technology, 61*(3), 287–292. https://doi.org/10.1016/j.seppur.2007.11.004

[9]. Kassem F.A.F., Alrawi O.M.A. (2008). New method for cheap production of urea phosphate. *Patent №. WO/2008/046428,18.*

[10]. Xie, T., Zhang, Q., Wang, S., Yang, F., Li, T., Liu, F., Shi, L. (2010). Method for producing urea phosphate by vacuum crystallization. Faming Zhuanli Shenqing Gongkai Shuomingshu. *Chinese patent. №. CN. 101665453:8.*

[11]. Mubarak, Y. (2011) Production of Crystalline Urea Phosphate using the Untreated Jordanian Wet Process Phosphoric Acid.Dirasat, *Engineering Sciences, 38*(1), 61–72.

[12]. Broodryk, P.A. (2019) *Reaction kinetics of the pyrolysis of urea phosphate*. Diss. North-West University.

[13]. Wezenberg, S., Vlatković, M., Kistemaker, J., Feringa, B. (2014). Multi-state regulation of the dihydrogen phosphate binding affinity to a light-and heat-responsive bis-urea receptor. *Journal of the American Chemical Society, 136.*(48), 16784–16787. https://doi.org/10.1021/ja510700j

[14]. de Jong, J., Feringa, B.L., Wezenberg, S.J. (2019) Light-Modulated Self-Blockage of a Urea Binding Site in a Stiff-Stilbene Based Anion Receptor. *Chem. Phys. Chem., 20*(4), 3306–3310. https://doi.org/10.1002/cphc.201900917

[15]. Zhao, J., Yang, D., Zhao, Y., Cao, L., Zhang, Z., Yang, X., Wu, B. (2016). Phosphate-induced fluorescence of a tetraphenylethene-substituted tripodal tris (urea) receptor. *Dalton Transactions. 45*(17), 7360–7365. https://doi.org/10.1039/C6DT00672H

[16]. Yerokun, O.A. (1997) Ammonia volatilization from ammonium nitrate, urea and urea phosphate fertilizers applied to alkaline soils. *South African Journal of Plant and Soil., 14*(2), 67–70. https://doi.org/10.1080/02571862.1997.10635084

[17]. Almog, J., Burda, G., Shloosh, Y., Abramovich-Bar, S., Wolf, E., Tamiri, T. (2007) Recovery and detection of urea nitrate in traces. *Journal of forensic sciences, 52*, 1284–1290 https://doi.org/10.1111/j.1556-4029.2007.00551.x

[18]. Oxley, J.C., Smith, J.L., Vadlamannati, S., Brown, A.C., Zhang, G., Swanson, D.S., Canino, J. (2013) Synthesis and characterization of urea nitrate and nitrourea. *Propellants, Explosives, Pyrotechnics, 38*(3), 335–344. https://doi.org/10.1002/prep.201200178

[19]. Mardonov, U.M., Kholikova, G.K., Ganiev, B.S., Tursunova, I.N., Khozhiev, S.T. (2023). Synthesis and study of the agrochemical properties of urea salts with nitric and orthophosphoric acid. *In E3S Web of Conferences, 389*, 03005. https://doi.org/10.1051/e3sconf/202338903005

[20]. Spaeth, N.J. (1943). Woodbury, Preparation of Nitrourea., E.I. du Pont de Nemours & Company, Wilmington DL, USA. *US Patent 2,279,765. C.P.*

[21]. Almog, J., Klein, A., Sokol, A., Sasson, Y., Sonenfeld, D., Tamiri, T. (2006). Urea nitrate and nitrourea: powerful and regioselective aromatic nitration agents. *Tetrahedron letters, 47*(49), 8651–8652. https://doi.org/10.1016/j.tetlet.2006.10.027

[22]. Amrullaev, A., Boltaeva, S., Rashitova, S., Ganiev, B. (2024). Synthesis and study sorption properties oligo (poly)-mer sorbents based on urea-formaldehyde and cyanuric acid. In BIO Web of Conferences. *EDP Sciences, 130*, 06004. https://doi.org/10.1051/bioconf/202413006004

[23]. Ermuratova, N.A., Turaev, K.K., Kornilov, K.N., Abduvalieva, M.Z., Chorieva, N.B. (2023). Adsorption Ability of Nitrogen-Containing Polymer Sorbents Based on Urea-Formaldehyde Resin and Aminoacetic Acid Towards Heavy Metal Ions. *Polymer Science, Series A, 65*(6), 666–671. https://doi.org/10.1134/S0965545X23600679

[24]. Nazarov, S., Amrieva, S., Ganiev, B., Nazarov, N. (2024). Synthesis and spectroscopic study of adhesive polymer materials based on urea-formaldehyde and isoamyl alcohol. *In BIO Web of Conferences, 130*, 06003. https://doi.org/10.1051/bioconf/202413006003

[25]. Abbasov, V., Abdullayev, E., Ismayilov, T., Hasanova, A., Alizadeh, R. (2023). Comparative study of complexes with different mole ratio of orthophosphoric acid and carbamide against corrosion and salt precipitation. *Processes of Petrochemistry and Oil Refining, 24*(4). https://doi.org/10.36719/1726-4685/96/656-665

[26]. Ganiyev, B.S., Sayfillayeva, D.K., Sharipov, M.S., Ramazanov, B.G. (2025). Synthesis and study of phsysico-chemical properties of oligo (poly)-mer sorbents based on urotropine and cyanuric acid. *Journal of Chemistry and Technologies, 33*(2), 391–400. https://doi.org/10.15421/jchemtech.v33i2.325935

[27]. Holikov, A.J., Akbarov, H.I., Tillaev, R.S. (2005). Protective properties of phosphoric acid-based inhibitors in various media. *Composite Materials*, (4), 18–20.

[28]. Eshmamatova, N. B., Akbarov, Kh. I., Rajabov, Yu. N., Khudoyqulova, R. Z., Sunatov, Sh. Sh., Bakhromov, I. A., Akhmedova, N. K. (2019). Protective efficiency of organic-type inhibitors based on urea. Composite *Materials*, (2), 355–359.

[29]. Doebelin, N., Kleeberg, R. (2015). Profex: a graphical user interface for the Rietveld refinement program BGMN. *Applied Crystallography, 48*(5), 1573–1580.

[30]. Eksperiandova, L.P., Fedorov, O.I., Stepanenko, N.A. (2011). Estimation of metrological characteristics of the element analyzer EuroVector EA-3000 and its potential in the single-reactor CHNS mode. *Microchemical journal, 99*(2), 235–238. https://doi.org/10.1016/j.microc.2011.05.005

[31]. Vetsner, Y.I. (2021). Urea phosphate as a component of complex NPCa-fertilizers. *Chemical problems of today*, 132–132.

[32]. Vetsner, Y. (2017). [Study of the process of obtaining urea phosphate]. *Bulletin of the National Technical University "KhPI". Series: New Solutions in Modern Technologies, 23*(1245), 137–143. https://doi.org/10.20998/2413-4295.2017.23.22

[33]. Baumer, V.N., Shishkin, O.V. (2011). [*X-ray diffraction methods for studying biologically active compounds. Analytical chemistry in the creation, standardization, and quality control of medicinal products*]. Khar'kov, "NTMT". (In Ukrainian)

[34]. Ghammamy, S., Hosseiny, N. M., Aghbolagh, Z. S., Sahebalzamanib, H. (2011). Extraction of Crystal structural data of a number of chromate use complexes by of Rietveld equation and WinPLOTR program from

powder diffraction patterns. *Archives of Applied Science Research, 3*(2), 25–28.

[35]. Lechs, M., Zundel, G. (1979). Polarizable acid-acid and acid-water hydrogen bonds with M, PO, H, PO, H_3PO_4, and HH, AsO, l. *Canadian Journal of Chemistry, 57*, 487–493. https://doi.org/10.1139/v79-080

[36]. Rudolph, W. W. (2010). Raman-and infrared-spectroscopic investigations of dilute aqueous phosphoric acid solutions. *Dalton Transactions, 39*(40), 9642-9653. https://doi.org/10.1039/C0DT00417K